

9. FERROMAGNETIC AND MATRIX SUSCEPTIBILITIES IN PLIOCENE–PLEISTOCENE HEMIPELAGIC MARLS FROM THE WESTERN MEDITERRANEAN SEA¹

Charles Aubourg,² Anne Murat,³ M. Torii,⁴ and Omar Oufi^{2,5}

ABSTRACT

We emphasize the importance of the matrix susceptibility of hemipelagic marls that have weak low-field susceptibility (K_o). In Hole 977A, the continuous record of K_o in the first 60 m below seafloor shows oscillations that are in good agreement with the oxygen isotopic data. This, therefore, suggests a record of climatic signal. The relevant relationship between K_o and NGR permits a semiquantitative estimate of the paramagnetic susceptibility, which is essentially the matrix susceptibility. We measured the high-field susceptibility of 63 samples from Holes 974B, 976C, and 977A and found that matrix susceptibility dominates K_o when $K_o < 300 \mu\text{SI}$ (10^{-6} SI units by volume). Both the matrix and ferromagnetic susceptibilities vary in the same proportion. This result is of major importance and cautions against the use of K_o as a normalizer in sediments for rock-magnetic paleointensity investigation. Hysteresis parameters and low-temperature demagnetization of isothermal remanent magnetization indicate the occurrence of chemically pure magnetite with pseudo–single-domain structure. We observed a progressive dissolution of magnetite with depth. Local enhancement of paramagnetic or superparamagnetic susceptibilities are observed at the top of organic-rich layers.

INTRODUCTION

Initial magnetic susceptibility (K_o), generally expressed in μSI (10^{-6} SI units by volume) is one of the most commonly used rock-magnetic parameters investigated because it can be easily and precisely obtained. K_o is widely used in rock magnetism (Dunlop, 1995), environmental magnetism (Verosub and Roberts, 1995), for determination of paleointensity (Valet and Meynadier, 1993), and for determination of magnetic fabric (Rochette et al., 1992). In hemipelagic marls, K_o has two principal sources: $K_o = K_f + K_p$, where K_f is the ferromagnetic susceptibility and K_p is the matrix susceptibility. The matrix has contributions from paramagnetic, diamagnetic, and antiferromagnetic susceptibilities. Rochette (1987) emphasized the importance of K_p in sediments and calculated a threshold where the relative importance of K_p and K_f varies. This threshold is $\sim 300 \mu\text{SI}$. Rochette proposed that the predominance of K_p is likely below this value and must be considered. K_o is commonly used as a proxy for K_f even for low-susceptibility clay sediments where K_p is not negligible. The importance of the matrix susceptibility in rock-magnetic investigations is outlined by Dekkers et al. (1994). They cautioned against the wide use of the ratio K_{ARM}/K_o (K_{ARM} is the anhysteretic susceptibility) introduced by Banerjee et al. (1981) to estimate relative grain-size variation. Dekkers et al. (1994) considered the importance of K_p and calculated an increase in K_{ARM}/K_o from 100 to 368 that is independent of grain size and is only caused by the relative enhancement of the matrix contribution K_p resulting from magnetite dissolution.

Several methods can be used to calculate the matrix susceptibility, including high magnetic-field measurements (Rochette et al., 1983), magnetic extraction (Henry and Daly, 1983), and thermal variation of K_o from liquid nitrogen to room temperature (Schultz-Krutisch and Heller, 1985). Thibal (1995) proposed to use natural gamma ray

(NGR) as a quick means to obtain K_p by considering the proportional relationship between NGR and clay content in marine sediments. Clays are responsible for almost the entire matrix susceptibility in marine sediments (Rochette, 1987). Thus, on the basis of the relevant relationship between the continuous record of K_o and NGR, Thibal successively derived K_p and K_f .

In this paper, we emphasize general features of the continuous record of magnetic susceptibility and NGR in marls from Hole 977A. We performed rock-magnetic investigations on 67 discrete samples from Holes 974B, 976C, and 977A to better understand the relative importance of matrix susceptibility and ferromagnetic grains.

RESULTS

Bulk Susceptibility vs. Depth in Hole 977A

A continuous record of the magnetic susceptibility in Hole 977A (Fig. 1; see Shipboard Scientific Party, 1996) shows different susceptibility patterns on different scales. Visible on a large scale are two zones of high K_o amplitude (0–80 and 420–540 meters below seafloor [mbsf]) separated by a quiet zone where the background value of K_o is ~ 50 – $100 \mu\text{SI}$. Similarly, NGR shows an opposite pattern, with low values restricted to the area of high K_o amplitudes. Two significant features are visible on a smaller scale in the magnetic susceptibility record:

1. The oscillation of K_o in the first 60 mbsf (Fig. 2) is independent of lithology and is likely related to a climatic signal as shown by the correspondence between peaks of K_o and *G. bulloides* oxygen isotopic data (von Grafenstein et al., Chap. 37, this volume). This suggests that peaks of K_o correspond to cold periods. Note also the relevant agreement between oscillations of NGR and K_o .
2. Organic-rich layers typically have low values of K_o ($< 100 \mu\text{SI}$). From Figure 2 (and more precisely on Fig. 3), one can see that the top of the organic-rich layers is commonly characterized by a peak in susceptibility. This K_o signature of organic-rich layers (Fig. 3) was monitored during the cruise to successfully detect organic-rich layers during the initial sedimentary description of the working half of the core. The dif-

¹Zahn, R., Comas, M.C., and Klaus, A. (Eds.), 1999. *Proc. ODP, Sci. Results*, 161: College Station, TX (Ocean Drilling Program).

²Department of Earth Sciences (URA 1759), Cergy Pontoise University, 95011 Cergy, France. Aubourg: aubourg@u-cergy.fr

³Intechmer, BP 324, 50103 Cherbourg cedex, France.

⁴Division of Earth and Planetary Sciences, Graduate School of Sciences, Kyoto University, Kyoto 606-01, Japan.

⁵Laboratoire de Pétrologie Métamorphique (URA 736), University Paris VI-VII, 11 Place Jussieu, 75252 Paris, France.

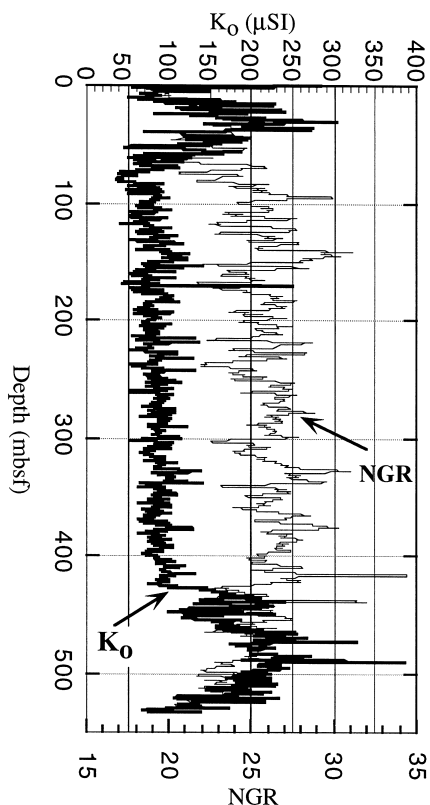


Figure 1. Initial magnetic susceptibility (K_o) and natural gamma-ray counts (NGR) vs. depth. Both K_o and NGR are smoothed (sliding window of 20 data points).

ference (Fig. 3) between the susceptibility of discrete samples and that recorded continuously using the magnetic susceptibility meter can be explained by the smoothing of the continuous values, which are effectively being filtered by the magnetic susceptibility meter. An alternative explanation could be late oxidation of the sediments.

Matrix Susceptibility

High-Field Magnetic Susceptibility

We performed hysteresis measurements on 63 samples using a translation inductometer designed by M. Le Goff (Geomagnetism Laboratory, Saint Maur, France). The maximum sensitivity is $\sim 2 \times$ DC) field of 2 T. The weight of samples (2 g) allows a reliable description of the ferromagnetic content. From the linear trend of the high-field magnetization, we derived the high-field magnetic susceptibility K_{hf} , which is a proxy for K_p , the matrix susceptibility. We measured initial susceptibility K_o on the same sample using the Kappabridge KLY-2, and calculated K_f the ferromagnetic susceptibility K_f (Table 1) by using the equation:

$$K_f = K_o - K_{hf}$$

When comparing the matrix contribution ($\%K_p = [K_p/K_o] \times 100$) vs. initial susceptibility K_o (Fig. 4), we obtain a good correlation for all but a few samples from Hole 977A. The paramagnetic contribution decreases according to a power law and is predominant below 300 μ SI, in good agreement with the limit proposed by Rochette (1987). The matrix contribution varies significantly below 300 μ SI; it ranges from 60% to 100% for $K_o = 160 \mu$ SI (Fig. 4).

Some samples are characterized both by high K_o and high matrix contribution. All these samples correspond to the K_o peak observed

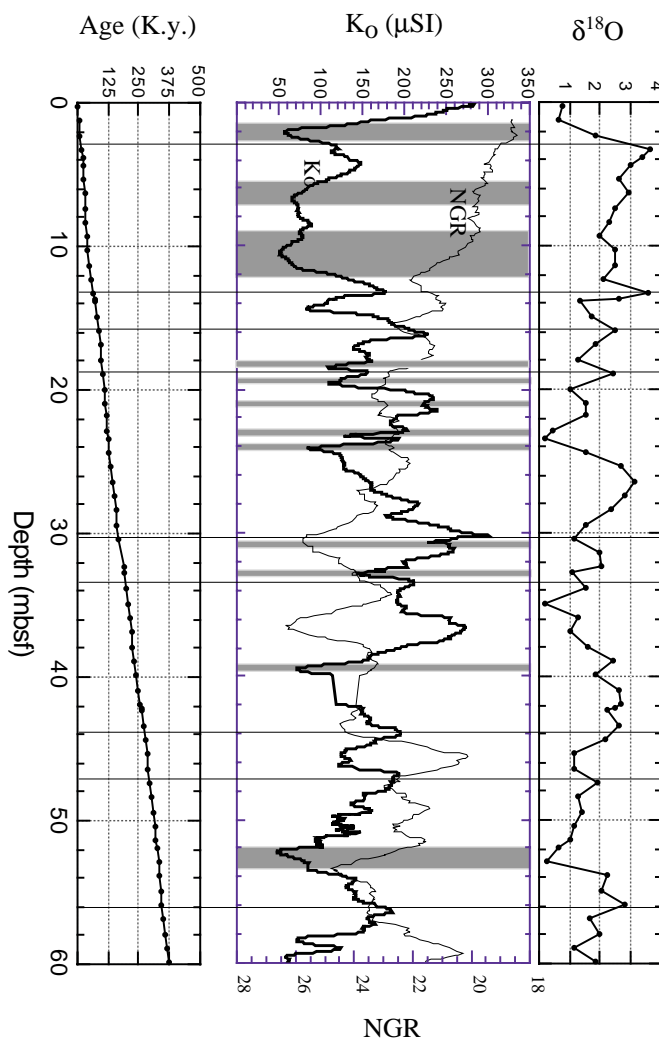


Figure 2. Initial magnetic susceptibility (K_o) and natural gamma-ray counts (NGR) vs. depth. Note that NGR is plotted on a reverse scale. Shaded boxes correspond to organic-rich layers (Shipboard Scientific Party, 1996). Oxygen isotope data (*G. bulloides*) and tuned age are also shown. Peaks in the $\delta^{18}O$ and K_o curves correspond to cold periods.

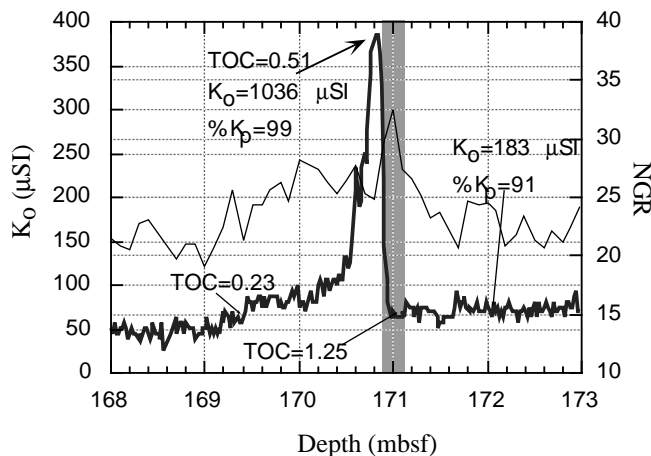


Figure 3. Detailed view of K_o and NGR from 168 to 173 mbsf. The top of the organic-rich layers (shaded band) is clearly associated with a peak in K_o . Discrete measurements, such as TOC values, K_o , and matrix susceptibility ratios ($\%K_p$), are reported.

Table 1. Magnetization, susceptibility, and hysteresis parameters at Holes 974B, 976C, and 977A.

Core, section, interval (cm)	Depth (mbsf)	K_o (μ SI)	K_p (μ SI)	K_f (μ SI)	% K_p ($[K_p/K_o] \times 100$)	J_s (10^{-3} Am ² /kg)	J_{rs} (10^{-3} Am ² /kg)	H_c (mT)	H_{cr} (mT)
161-974B-									
1H-2, 214-216	2.64	569	194	375	34	49	9	13	36
2H-2, 62-64	8.62	439	152	287	35	39	6	11	36
2H-5, 85-87	13.35	300	183	117	61	27	5	12	34
2H-6, 100-102	15.00	324	183	140	57	31	7	14	36
3H-1, 91-93	16.91	186	132	54	71	19	4	12	34
3H-2, 24-26	17.74	349	161	188	46	22	5	12	34
3H-2, 125-127	18.75	164	138	26	84	13	3	13	36
3H-3, 120-122	20.2	370	183	187	50	23	4	12	35
4H-1, 116-118	26.66	419	174	244	42	29	6	13	35
4H-5, 128-130	32.78	318	109	209	34	27	6	14	33
5H-2, 118-120	37.68	246	175	70	71	14	3	11	37
5H-3, 127-129	39.27	219	195	24	89	13	3	14	38
5H-4, 138-140	40.88	314	181	133	58	17	3	11	36
7H-2, 35-37	55.56	375	143	232	38	28	5	12	33
7H-5, 124-126	60.95	168	144	24	86	6	1	10	37
8H-6, 110-112	72.00	216	162	53	75	7	2	10	36
9H-2, 24-26	74.74	257	142	116	55	12	2	11	33
9H-5, 84-86	79.74	176	177	-0	100	10	2	10	36
10H-6, 19-21	89.89	185	159	26	86	6	2	11	36
13H-2, 110-112	113.6	130	142	-0	100	6	2	15	61
14H-2, 120-122	123.2	150	113	37	76	7	2	11	34
14H-3, 25-27	123.75	188	120	68	64	8	2	13	35
14H-5, 120-122	127.7	187	138	49	74	8	2	12	46
16H-2, 120-122	142.2	187	152	35	81	6	1	9	38
17H-1, 30-32	149.3	114	100	15	87	3	1	9	35
18H-1, 235-27	158.75	268	169	99	63	6	1	9	37
18H-1, 110-112	159.6	216	179	37	83	8	2	10	33
18H-3, 110-112	162.6	150	130	21	86	4	1	12	39
18H-5, 28-30	164.78	168	126	42	75	4	1	13	41
19X-1, 133-135	166.33	172	131	42	76	6	1	10	37
19X-3, 137-139	169.37	239	156	83	65	7	2	10	36
19X-5, 19-21	171.19	150	142	9	94	4	1	9	43
20X-5, 31-33	181.2	204	190	15	93	5	1	9	38
22X-5, 16-18	200.26	317							
22X-6, 6-8	201.66	294	211	84	72	9	1	5	31
161-976C-									
4H-1, 11-13	25.11	968	251	716	26	15	3	12	26
4H-2, 110-112	27.60	249	202	47	81	2	<1	8	16
4H-3, 123-125	29.93	349	212	137	61	6	1	12	
4H-4, 126-128	30.76		255			14	3	12	29
4H-6, 50-52	33.00	254	194	60	76	3	<1	8	16
5H-2, 5-7	36.05	590	236	354	40	11	3	14	
5H-3, 10-12	37.60	298	191	107	64	4	1	11	23
5H-4, 43-45	39.43	572	231	341	40	12	3	16	
5H-5, 27-29	40.77	233	190	43	82	1	0	6	
15X-1, 57-59	130.07	396	350	46	88				
15X-1, 90-92	130.40	218	167	51	77				
161-977A-									
3H-2, 130-132	16.30	1093	233	860		16	4	12	
3H-4, 27-29	18.27	647	132	514		9	2	14	33
3H-4, 48-50	18.48	261	132	129					
4H-5, 145-147	30.45	735	249	486		15	4	15	37
4H-6, 2-4	30.52	424	199	225		6	1	16	42
17H-5, 129-131	153.79	996	949	48					
17H-6, 2-41	54.02	192	132	59					
18X-1, 13-15	156.13	761	665	96					
18X-3, 9-10	159.09	633	633	0					
18X-3, 14-16	159.14		334						
18X-6, 14-16	163.64	809	808	1					
19X-4, 73-75	170.83	1036	1033	3					
19X-5, 60-62	172.20	183	167	16					
24X-1, 147-149	215.07	1274	933	341					
47X-3, 110-112	439.00	526	167	359	14	4	14	28	
48X-4, 23-25	449.25	183	167	897	25	3	9		
52X-5, 88-90	489.78	502	117	385	12	2	11	30	
56X-6, 18-20	529.08	2828	299	2828	90	12	10	31	

Notes: K_o = Initial magnetic susceptibility, K_p = matrix susceptibility, K_f = ferromagnetic susceptibility, J_s = saturation magnetization, J_{rs} = remanent magnetization, H_c = coercive field, and H_{cr} = remanent coercive field obtained from investigations of hysteresis parameters.

just above the organic-rich layers in Hole 977A (Fig. 3). Such high matrix susceptibilities can result either from superparamagnetic ferromagnetic grains, from paramagnetic minerals, or from a combination of both. X-ray analysis indicates the occurrence of siderite (FeCO₃; Shipboard Scientific Party, 1996), which has a relatively high antiferromagnetic susceptibility. We measured initial susceptibilities of ~4000 μ SI on single 6-cm³ crystals (Shipboard Scientific Party, 1996). The value of K_o = 1000 μ SI above the organic-rich layers suggests at least 20% by volume of siderite, which is unlikely in marine marls, which generally contain <1% (Baker and Burns, 1985).

Moreover, the magnetic fabric from a few samples is normal (i.e., with the direction of minimum susceptibility [K_s] perpendicular to the bedding; Shipboard Scientific Party, 1996). This argues against high siderite abundance, which would result in an inverse magnetic fabric (i.e., K_s within the bedding plane; Ellwood et al., 1986; Rochette, 1988).

The matrix contribution increases significantly with depth (Fig. 5A). Below 60 mbsf, the matrix contribution is dominant. Below 400 mbsf in Hole 977A, the ferromagnetic susceptibility again plays a major role without a significant change in lithology.

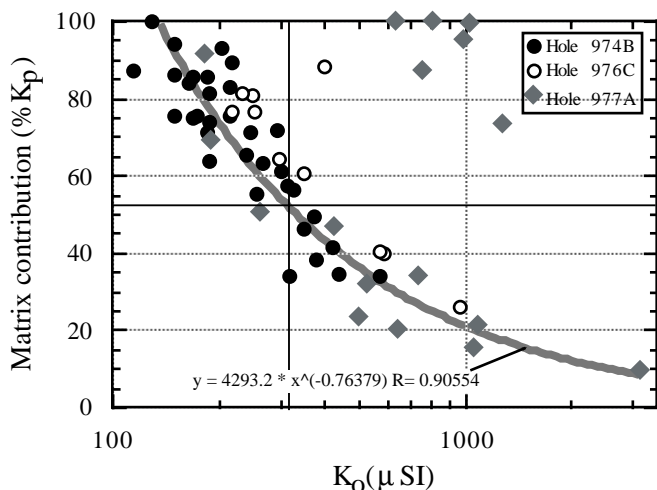


Figure 4. Matrix contribution ($\%K_p = 100 \times [K_p/K_o]$) vs. initial susceptibility K_o .

Natural Gamma Ray as a Proxy of Matrix Susceptibility

The relationship between oscillation of K_o and NGR is clearly expressed in Figures 1–3. In Hole 977A, the matrix contribution correlates well with the magnitude of NGR, to a first approximation. NGR ranges from 20 to 25 for a matrix contribution <50%, and from 25 to 30, when matrix contribution is dominant (Fig. 1). It is now questionable whether NGR is directly proportional to the matrix susceptibility. In Hole 977A, K_o is mostly of paramagnetic origin between 100 and 400 mbsf. When comparing K_o with NGR (Fig. 6A), a one-to-one relationship is observed between peaks, although the relationship between the magnitudes of K_o and NGR is poor (Fig. 6B).

Characterization of the Ferromagnetic Grains

Low-Temperature Susceptibility Curves

We analyzed the low-temperature (5 K–300 K) demagnetization of isothermal remanent magnetization (IRM) by using a susceptibility meter on a multisensor track (Low-Temperature Laboratory of Kyoto University). IRM was imparted at 1 T after cooling the sample at 5 K. We measured five samples from between 16.30 and 30.52 mbsf in Hole 977A (Fig. 7). A significant change of slope at ~110 K indicates the Verwey transition and the occurrence of chemically pure magnetite (Özdemir et al., 1993). Torii (1997) has extended the low-temperature investigation of Site 977 by making 74 additional measurements and found Verwey transitions at depths ranging from 1 to 56 mbsf. Below 56 mbsf, the Verwey transition is not clearly detectable. The continuous decay of IRM from 100 K to 300 K suggests the presence of appreciable amounts of ultrafine magnetites in the superparamagnetic domain (Hunt et al., 1995). In addition, the sharp drop of IRM at ~30–40 K could represent pyrrhotite (Rochette et al., 1990) or siderite (Housen et al., 1996) transitions.

Hysteresis Parameters

From hysteresis curves, we derived saturation magnetization (J_s), remanent saturation magnetization (J_{rs}), coercive field (H_c), and remanent coercive field (H_{cr}) when the ferromagnetic signal was fairly identifiable (Table 1). Use of the Day diagram (Day et al., 1977) of J_{rs}/J_s vs. H_{cr}/H_c (Fig. 8) places the magnetites in the pseudo-single-domain structure. In Hole 974B, the rough increase of H_{cr}/H_c from 2 to ~5 with depth (Fig. 5B) suggests a progressive enhancement in the contribution of superparamagnetic grains.

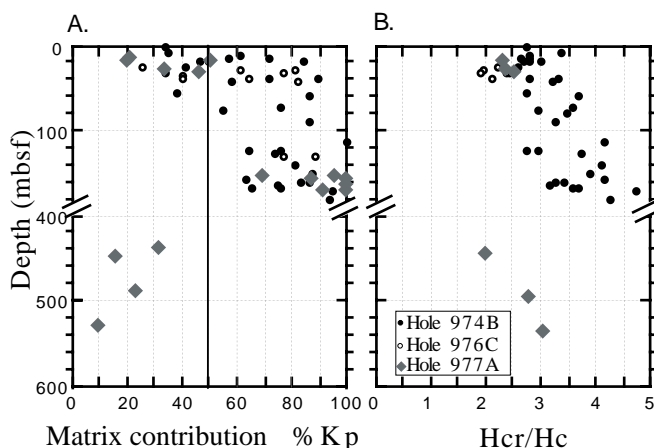


Figure 5. A. Matrix contribution ($\%K_p = 100 \times [K_p/K_o]$) vs. depth. B. Ratio of coercive field H_{cr}/H_c vs. depth. Note the nonlinear depth scale.

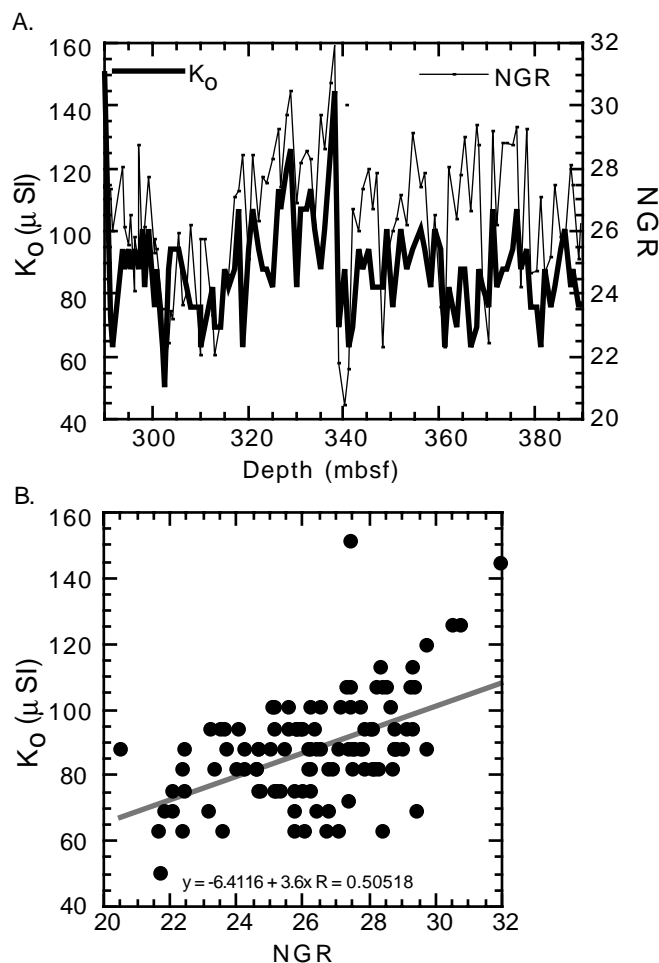


Figure 6. A. NGR and K_o vs. depth for Hole 977A. B. K_o vs. NGR magnitude. Note the close correspondence of peaks (A) and the poor relationship with magnitude (B).

DISCUSSION

Our results emphasize the importance of the matrix contribution in marls of the Alboran and Tyrrhenian Seas. First, we have shown

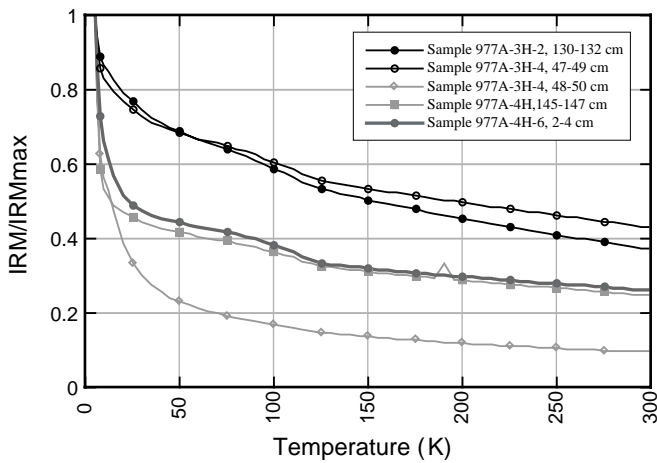


Figure 7. Low-temperature (5–300 K) demagnetization of isothermal remanent magnetization (IRM). The Verwey transition at 114 K indicates the presence of multidomain to pseudo-single-domain magnetites. The drop of IRM below 50 K could be attributed to a pyrrhotite or siderite transition. The decay of IRM after 150 K could be attributed to superparamagnetic grains (magnetites or iron sulfides).

that the matrix contribution decreases when K_o increases, following roughly a power law (Fig. 4). Below 300 μSI , K_p is $>K_f$ and varies in the same proportion. Thus, the variation of K_o below 300 μSI could be caused by the input of both ferromagnetic and paramagnetic grains. This has important implications for the use of K_o as a standard normalizer for paleointensity determinations (King et al., 1983) or grain-size variations when K_o is combined with anhysteretic susceptibility. Second, we observed evidence of magnetite dissolution with depth. This is suggested by the following:

1. An increase in the matrix contribution with depth (Fig. 5A). Below 60 mbsf, the matrix dominates the susceptibility signal in Holes 974B, 977A, and 976C. This result is consistent with the progressive magnetite dissolution and subsequent pyritization with depth found at Site 653, 50 km away from Site 974 (Channel and Hawthorne, 1990).
2. The increase of H_{cr}/H_c with depth observed in Hole 974B supports a relative enhancement of superparamagnetic grains.
3. A systematic absence of Verwey transition below 56 mbsf in Hole 977A (Torii, 1997).

The relative importance of K_p can be quickly appreciated by comparing NGR and K_o data, as proposed by Thibault (1995). In the first 60 mbsf of Hole 977A, the close correspondence between NGR and K_o oscillations, as well as relevant matches with oxygen isotopic data peaks (Fig. 2), suggests that susceptibility variations are climatically driven forces and that relative changes in both matrix and ferromagnetic susceptibilities play a role. However, the magnitude of NGR is not directly proportional to K_o (Fig. 6B). This negates a priori the discrimination of K_p and K_f by using only NGR and K_o data (Thibault, 1995).

Another significant result of this study is the susceptibility signature observed in the organic-rich layers. High total-organic-carbon sediments are characterized by weak susceptibility ($\sim 100 \mu\text{SI}$ and below) and natural remanent magnetization (10^{-5} to 10^{-3} A/m; Shipboard Scientific Party, 1996), as already found by Dekkers et al. (1994) in sapropel layers from the Central Mediterranean. In addition, we observed that the tops of organic-rich layers in Hole 977A are characterized by a distinguishable peak of paramagnetic susceptibility up to 1000 μSI . The source of this strong paramagnetic sus-

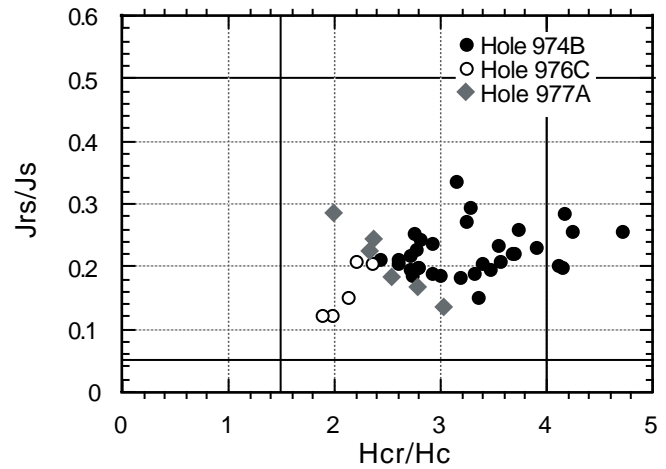


Figure 8. Hysteresis parameter ratios J_{rs}/J_s vs. H_{cr}/H_c .

ceptibility is probably ultrafine magnetites or iron sulfides in the superparamagnetic state. Siderite is also a candidate to account for a small part of this strong paramagnetic signal.

The increase of ferromagnetic grains below 420 mbsf in Hole 977A, as exemplified by higher K_o and K_p , starts at ~ 3 Ma on the basis of biostratigraphic data (Shipboard Scientific Party, 1996). This can be related to a late Neogene volcanism event (Bellon et al., 1983) and subsequent input of magnetites.

CONCLUSIONS

A record of K_o in Hole 977A provides a good opportunity to evaluate the importance of the matrix contribution. Significant results are the following:

1. Matrix contribution is dominant for $K_o < 300 \mu\text{SI}$.
2. Matrix and ferromagnetic susceptibilities vary in a similar way when $K_o < 300 \mu\text{SI}$.
3. Matrix contribution increases with depth down to 400 mbsf, which suggests progressive ferromagnetic grain dissolution. These results, therefore, caution against the use of K_o as a ferromagnetic susceptibility proxy when $K_o < 300 \mu\text{SI}$. The progressive ferromagnetic dissolution observed in Hole 977A can significantly obscure relative paleointensity changes if NRM/K_o is used.
4. To quickly estimate the matrix contribution, we propose a comparison between oscillations and magnitude of natural gamma rays and initial susceptibility. A good agreement in both cases supports a high matrix contribution as well as significant variation of K_p . An absence of magnitude relationship is inconclusive.
5. The organic-rich layers are characterized by low susceptibilities, which suggests anoxic conditions.
6. A strong paramagnetic susceptibility peak observed above the organic-rich layers provides a consistent susceptibility signature for the organic-rich layers. Principal sources of the susceptibility peak are superparamagnetic magnetites and possibly siderites.
7. Preliminary isotopic data confirm that K_o oscillations are driven by climatic forces in the first 60 mbsf of Hole 977A, and probably below. In particular, K_o peaks seem to be related to cold periods.

This confirms the high capability of hemipelagic sediments of the Alboran Basin to record climatic signals. Thus, future work will be directed toward the recognition of climate-driven forces by studying the continuous susceptibility records and isotopic data from the Alboran Sea (Holes 976C, 977A, and 979A).

ACKNOWLEDGMENTS

The authors benefited from open and stimulating discussion with the scientific team during the cruise. We are pleased to acknowledge M. Hobart, R. Wilkens, M. Prasad, and K. Tandon, who kindly provided fresh records of magnetic susceptibility during the cruise. Thanks to R. Zahn who recognized the importance of organic-rich layers in the Alboran Sea and froze the samples. C.A. addresses special thanks to J.P. Pozzi for discussions on the use of NGR and magnetic susceptibility. M. Fuller and B. Housen helped greatly with the clarity and science of this paper.

REFERENCES

- Baker, P.A., and Burns, S.J., 1985. The occurrence and formation of dolomite in organic-rich continental margin sediments. *AAPG Bull.*, 69:1917–1930.
- Banerjee, S.K., King, J.W., and Marvin, J., 1981. A rapid method for magnetic granulometry with application to environmental studies. *Geophys. Res. Lett.*, 8:333–336.
- Bellon, H., Bordet, P., and Montecat, C., 1983. Chronologie du magmatisme néogène des Cordillères bétiques (Espagne méridionale). *Bull. Soc. Geol. Fr.* 7:205–217.
- Channell, J.E.T., and Hawthorne, T., 1990. Progressive dissolution of titanomagnetites at ODP Site 653 (Tyrrhenian Sea). *Earth Planet. Sci. Lett.*, 96:469–480.
- Day, R., Fuller, M., and Schmidt, V.A., 1977. Hysteresis properties of titanomagnetites: grain-size and compositional dependence. *Phys. Earth Planet. Inter.*, 13:260–267.
- Dekkers, M.J., Langereis, C.G., Vriend, S.P., van Santvoort, P.J.M., and De Lange, G.J., 1994. Fuzzy *c*-means cluster analysis of early diagenetic effects on natural remanent magnetization acquisition in a 1.1 Myr piston core from the Central Mediterranean. *Phys. Earth Planet. Inter.*, 85:155–171.
- Dunlop, D.J., 1995. Magnetism in rocks. *J. Geophys. Res.*, 100:2161–2174.
- Ellwood, B.B., Balsam, W., Burkart, B., Long, G.J., and Buhl, M.L., 1986. Anomalous magnetic properties in rocks containing the mineral siderite: paleomagnetic implications. *J. Geophys. Res.*, 91:12779–12790.
- Henry, B., and Daly, L., 1983. Séparations d'anisotropie magnétiques composantes en vue d'applications de l'étude quantitative de la déformation des roches. *C.R. Acad. Sci. Ser. 2*, 153:153–156.
- Housen, B.A., Banerjee, S.K., and Moskowitz, B.M., 1996. Low-temperature magnetic properties of siderite and magnetite in marine sediments. *Geophys. Res. Lett.*, 23:2843–2846.
- Hunt, C.P., Banerjee, S.K., Han, J.-M., Solheid, P.A., Oches, E.A., Sun, W.-W., and Liu, T.-S., 1995. Rock-magnetic proxies of climate change in the loess-paleosol sequences of the western Loess Plateau of China. *Geophys. J. Int.*, 123:232–244.
- King, J.W., Banerjee, S.K., and Marvin, J., 1983. A new rock-magnetic approach to selecting sediments for geomagnetic paleointensity studies: application to paleointensity for the last 4000 years. *J. Geophys. Res.*, 88:5911–5921.
- Özdemir, Ö., Dunlop, D.J., and Moskowitz, B.M., 1993. The effect of oxidation on the Verwey transition in magnetite. *Geophys. Res. Lett.*, 20:1671–1674.
- Rochette, P., 1987. Magnetic susceptibility of the rock matrix related to magnetic fabric studies. *J. Struct. Geol.*, 9:1015–1020.
- , 1988. Inverse magnetic fabric carbonate bearing rocks. *Earth Planet. Sci. Lett.*, 90:229–237.
- Rochette, P., Fillion, G., Mattéi, J.-L., and Dekkers, M.J., 1990. Magnetic transition at 30–34 Kelvin in pyrrhotite: insight into a widespread occurrence of this mineral in rocks. *Earth Planet. Sci. Lett.*, 98:319–328.
- Rochette, P., Fillion, G., Mollard, P., and Vergne, R., 1983. Utilisation d'un magnétomètre à effet Josephson pour l'analyse de l'anisotropie magnétique des roches. *C. R. Acad. Sci. Ser. 2*, 296:557–559.
- Rochette, P., Jackson, M., and Aubourg, C., 1992. Rock magnetism and the interpretation of anisotropy of magnetic susceptibility. *Rev. Geophys.*, 30:209–226.
- Schultz-Krutisch, T., and Heller, F., 1985. Measurement of magnetic susceptibility in Buntsandstein deposits from Southern Germany. *J. Geophys.*, 57:51–58.
- Shipboard Scientific Party, 1996. Site 977. In Comas, M.C., Zahn, R., Klaus, A., et al., *Proc. ODP, Init. Repts.*, 161: College Station, TX (Ocean Drilling Program), 299–353.
- Thibal, J., 1995. Analyse de l'aimantation des sédiments par diagrammes magnétiques, magnétostratigraphie, cyclicités climatiques et intensité du champ géomagnétique [Thesis]. Orsay Univ.
- Torii, M., 1997. Low-temperature oxidation and subsequent downcore dissolution of magnetite in deep-sea sediments, ODP Leg 161 (Western Mediterranean). *J. Geomagn. Geoelect.*, 49: 1233–1245.
- Valet, J.-P., and Meynadier, L., 1993. Geomagnetic field intensity and reversals during the past four million years. *Nature*, 336:234–238.
- Verosub, K.L., and Roberts, A.P., 1995. Environmental magnetism: past, present, and future. *J. Geophys. Res.*, 100:2175–2192.

Date of initial receipt: 7 May 1997
Date of acceptance: 9 January 1998
Ms 161SR-270